DYNAMIC RESPONSE OF COPPER SUBJECTED TO QUASI-ISENTROPIC, GAS-GUN DRIVEN LOADING

H. Jarmakani, J. M. McNaney, M. S. Schneider,
D. Orlikowski, J. H. Nguyen, B. Kad, M. A. Meyers

October 6, 2005

Disclaimer

This document was prepared as an account of work sponsored by an agency of the United States Government. Neither the United States Government nor the University of California nor any of their employees, makes any warranty, express or implied, or assumes any legal liability or responsibility for the accuracy, completeness, or usefulness of any information, apparatus, product, or process disclosed, or represents that its use would not infringe privately owned rights. Reference herein to any specific commercial product, process, or service by trade name, trademark, manufacturer, or otherwise, does not necessarily constitute or imply its endorsement, recommendation, or favoring by the United States Government or the University of California. The views and opinions of authors expressed herein do not necessarily state or reflect those of the United States Government or the University of California, and shall not be used for advertising or product endorsement purposes.

DYNAMIC RESPONSE OF COPPER SUBJECTED TO QUASI-ISENTROPIC, GAS-GUN DRIVEN LOADING

H. Jarmakani[1], J. M. Mc Naney[2], M. S. Schneider[1], D. Orlikowski[2], J. H. Nguyen[2], B. Kad[1], M. A. Meyers[1].

[1]*Mechanical and Aerospace Engineering Dept, Materials Science Program, University of California, San Diego, La Jolla CA 92093 0418*
[2]*Lawrence Livermore National Laboratory, Livermore CA 94550*

Abstract. A transmission electron microscopy study of quasi-isentropic high-pressure loading (peak pressures between 18 GPa and 52 GPa) of polycrystalline and monocrystalline copper was carried out. Deformation mechanisms and defect substructures at different pressures were analyzed. Current evidence suggests a deformation substructure consisting of twinning at the higher pressures and heavily dislocated laths and dislocation cells at the intermediate and lower pressures, respectively. Evidence of stacking faults at the intermediate pressures was also found. Dislocation cell sizes decreased with increasing pressure and increased with distance away from the surface of impact.

INTRODUCTION

Quasi-isentropic compression experiments (ICE) have been carried out since the early seventies. The main motivation behind such experiments was to simulate conditions occurring in the depths of planets. Entropy, the measure of the randomness of a system, does not change with depth in planets. Only temperature and pressure changes are experienced. As such, quasi-isentropic experiments come very close to replicating such conditions. Today, the interest behind these shockless experiments is focused on their ability to maintain the solid state of a material while it undergoes extreme pressures. The temperature rise during isentropic compression is significantly less severe than during shock compression. The solid state of a material can, thus, be retained, and an understanding and characterization of its response is possible.

Quasi-isentropic compression conditions can be achieved by various methods: gas-gun, laser, and magnetic loading. Early work on ICE with gas-gun by Lyzenga et al. [1] used a composite flyer plate with materials of increasing shock impedance away from the target material. Barker [2] placed powders of varying densities along a powder blanket and pressed the blanket to produce a pillow impactor having a smooth shock impedance profile. In the case of ICE via laser, McNaney et al. [3] used a shockless laser drive setup to compress and recover an Al alloy. A smoothly rising pressure pulse is generated by focusing a laser beam on a reservoir material (carbon foam), creating a plasma that "stretches out" through a vacuum and discharges onto the sample. In the case of magnetically driven experiments [4], the Z accelerator at Sandia National Labs (SNL) is capable of producing quasi-isentropic compression loading of solids using magnetic pulses. An advantage of this method is that a smoothly rising pressure profile can be generated without the initial spike at low pressures seen during impact experiments. Control

over loading pressures and a rise time is also possible to meet experimental requirements [4].

In this work, monocrystalline and polycrystalline copper samples were quasi-isentropically loaded via gas-gun. Peak pressures obtained ranged between 18 GPa and 51 GPa.

EXPERIMENTAL PROCEDURE

The two-stage gas gun and experimental set up for this work is located at LLNL. Functionally-graded material (FGM) impactors designed with increasing density profile or shock impedance, as depicted in Figure 1 below, were used to produce the smoothly rising pressure profiles [5].

Functionally Graded Material (FGM) Impactor　　**Target**
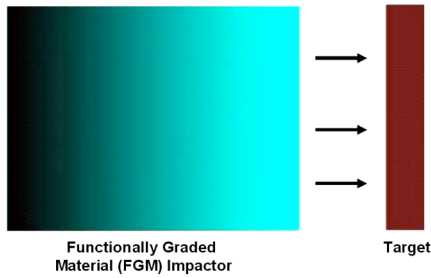
**Figure 1.** Illustration of FGM impactor hitting a target (darkness proportional to density).

The pressure profiles in Fig. 2 were obtained from simulations (CALE) carried out at LLNL. Five experiments, **A** (1700m/s), **B** (1260 m/s), **C** (730m/s), **D** (1760 m/s) and **E**, were carried out, with **A** experiencing the highest pressure of 51.5 GPa and **C** experiencing the lowest pressure of 17.7 GPa. Two distinct pressure profiles were attained, one having a hold-time of approximately 10 µsec and one having no hold time (or a "short pulse"). The as-received samples belonging to each batch were in the form of cylindrical specimens having an average diameter and thickness of 6mm and 3.6 mm, respectively.

Shock experiments are dictated by the following Swegle-Grady expression:

$$\dot{\varepsilon} = 7.84 \times 10^{-33} \times P^4 \qquad (1)$$

Where as the isentropic experiments have the following relationship:

$$\dot{\varepsilon} = 6.72 \times 10^{-9} \times P^{1.21} \qquad (2)$$
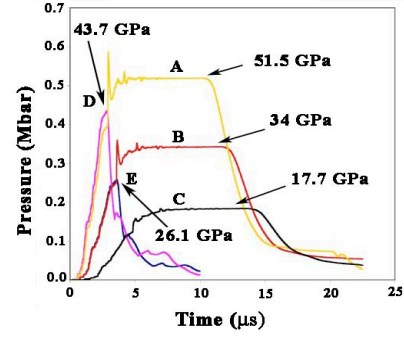
Figure 2. Pressure profiles of ICE experiments.

The figure below shows the strain rate versus pressure plot for these ICE experiments. Strain rates achieved during these ICE experiments are on the order of 10^4/sec, 10^4 to 10^5 orders of magnitude lower than shock experiments.
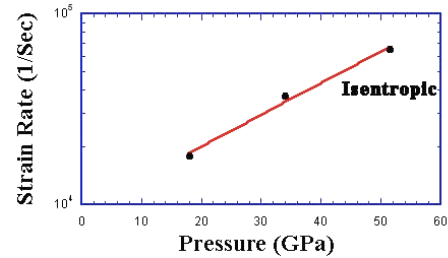
Figure 3. Strain Rate Vs. Pressure for ICE.

Grain Size and Micro-Hardness Measurements

Monocrystalline and polycrystalline samples in each batch were identified by macro-etching the bottom surface of the samples. The average grain size of the polycrystalline samples was approximately 36 µm. Microhardness measurements were performed on a selected group of samples (**A**, **B** and **C**). The top surface was indented using a Vickers tip attached to a Leco: M-400-H1 microhardness machine. The load applied was 200 gF, with a hold time of 15 sec.

TEM Sample Preparation

Cylindrical cuts having a diameter of 3mm through the center of each specimen were made by EDM. Four TEM foils were then sliced from each cylinder. The foils were electropolished and sent to Oak Ridge National Labs, where TEM was

performed under the SHaRE program. TEM analysis was performed on monocrystalline samples of experiments **A**, **B** and **C** and polycrystalline samples of experiments **C** and **D**.

RESULTS AND DISCUSSION

Microhardness Results

The hardness value increased from 103 KgF/mm^2 to 111 KgF/mm^2 with increasing pressure from 18 GPa to 52 GPa. An interesting trend was noticed in the monocrystalline samples. Hardness increased from **A** to **B,** but then dramatically decreased in **C**. The plot below shows this phenomenon. It is hypothesized that this behavior could be due to orientation effects within the crystals or melting on the impact surface, causing a decrease in hardness.
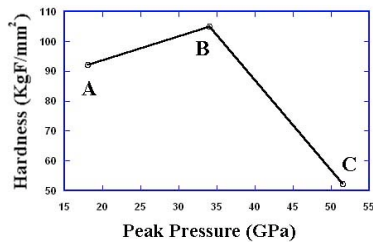

Figure 4. Hardness plot of monocrystalline samples.

TEM Results
*Monocrystalline Samples*

A sample from **A**, 51.5 GPa, located at 97µm from the impact surface contained very clear twinned regions, as can be seen from Figure 5. Both small and large twins were observed. A diffraction pattern revealed twinning taking place at the [011] orientation. At 1.2 mm from the surface within the same sample, a large concentration of dislocation cells, with an average size of 0.154 µm was observed. At 1.7 mm into the sample, heavy dislocation activity was evident, with dislocation cells of 0.198 µm. Twinning was still evident as well.

A monocrystalline sample from C, 18 GPa, revealed mostly dislocation activity, with cell sizes ranging in size from 0.5 µm at 0.13 mm within the sample to 0.65 µm at 1.9 mm within the sample.
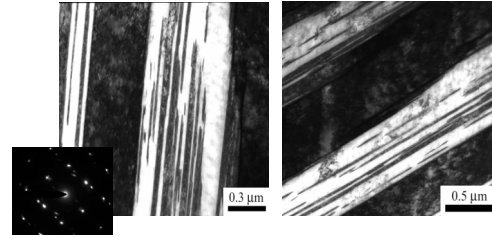
Figure 5. Twinned region at 97µm from the surface at a [011] orientation (experiment **A**).

The orientation of this crystal was determined to be [001]. An interesting feature within the top-most sample should be noted. Elongated cells were evident, but their sizes could not be discerned due to the limitations of the TEM pictures. It is not know whether these features are due to residual deformation or cratering introduced during specimen preparation. Figure 6 below shows typical dislocation activity found within this sample. The section is at 0.13 mm from the impact surface.
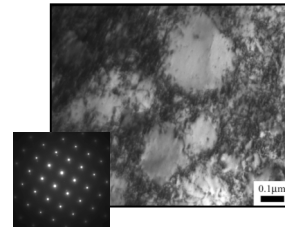

Figure 6. Dislocation cells at 0.13 mm form surface at [001] orientation (experiment **C**).

Analysis of a sample from **B** confirmed that the deformation at this intermediate pressure of 34 GPa was transitional, between **A** and **C**, as should be expected. Dislocation cells were mostly revealed at this pressure. Dislocation cell sizes at only two distances were determined, with sizes of 0.26 µm at 0.13 mm and 0.29µm at 0.74 mm.
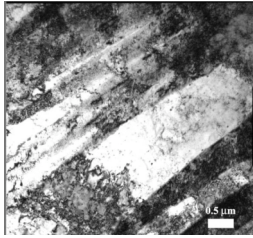
Polycrystalline Samples

A polycrystalline sample from **D** revealed heavily dislocated lathes at 0.14 mm from the top surface, as seen in Figure 7 (a). Dislocation cells and elongated dislocation features, Figure 7 (b), were evident further into the sample, specifically 1.3 mm from the surface, and irregular dislocation activity was evident at 1.9 mm from the surface.

(a)   **(b)**
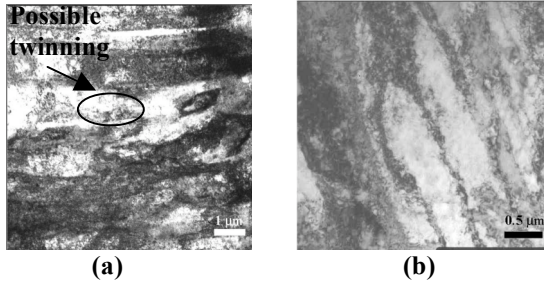
Figure 7. (a) Heavily dislocated laths with possible twinning at 0.14 mm, (b) Elongated cells at 1.3 mm (experiment **D**).

The polycrystalline sample from **C** revealed more dislocation cells. An interesting feature was exposed, hinting at stacking faults and heavily dislocated laths. The distance from the impact surface is unknown since this sample was prepared at LLNL. The figure below reveals this feature.


Figure 8. Stacking faults and Dislocated Laths (from **C**).

CONCLUSIONS

The deformation substructure is consistent with what is expected of impact treatment. In the case of the highest pressure, twinning in the monocrystalline sample was evident closest to the impact surface, and dislocation activity decreased with increasing distance from the impact surface for all experiments. This is consistent with work carried out by Schneider et al. [6] on laser shock of copper. It can be concluded that the twinning threshold lies between 34 GPa and 51 GPa. This is higher than in shock compression (~25 GPa). It is also noticed that the cell sizes achieved in ICE are larger than those of shock. In the case of the polycrystalline samples, heavily dislocated laths, regular, irregular and elongated dislocation features were evident. Evidence of staking faults was even

noticeable at the low pressure of 17.7 GPa. The plot below summarizes the change in cell size with distance for the various pressures considered.
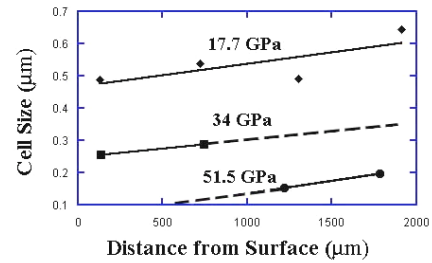
Figure 9. Cell-Size vs. Distance from impact surface.

REFERENCES

1. Lyzenga, G. A., and Ahrens, T. J., "One-Dimensional Isentropic Compression," in Shock Waves in Condensed Matter, 1981, W. J. Nellis, L. Seaman, and R. A. Graham, Eds., American Institute of Physics Conf. Proceedings No. 78 (1982) 231-235.
2. Barker, L. M., "High Pressure Quasi-Isentropic Impact Experiments", Shock Waves in Condensed Matter, 1984, J.R. Asay, R. A. Graham, and G. K. Straub, Eds., (Elsevier Sci. Pub., Amsterdam).
3. McNaney, J. M., Edwards, M. J., Becker R., Lorenz K. T., Remington B. A., "High Pressure, Laser Driven Deformation of an Aluminum Alloy," Met. Trans A, 35A, pp 265 (2004).
4. Hall, C. A. et al., "Experimental Configuration for Isentropic Compression of Solids using Pulsed Magnetic Loading", Review of Scientific Instruments, 72, 3587 (2001).
5. Nguyen. J.H. et al., "Specifically Prescribed Dynamic Thermodynamic Paths and Resolidification Experiments, Shock Compression of Condensed Matter, M. D. Furnish, L.C. Chhabildas, and R. S. Hixson, Eds., AIP Conf. Proc., Melville, New York (2004).
6. M.S. Schneider et al, "Laser-Induced Shock Compression of Copper: Orientation and Pressure Decay Effects." Met Trans A, 35 A, 263 (2004).